Chemical Engineering Journal 331 (2018) 744–754

Contents lists available at ScienceDirect

Chemical Engineering Journal

journal homepage: www.elsevier.com/locate/cej

Fabrication of high performance superhydrophobic coatings by spray-coating of polysiloxane modified halloysite nanotubes

Keying Feng[1], Guang-Yu Hung[1], Jiashang Liu, Mingqing Li, Changren Zhou, Mingxian Liu*

Department of Materials Science and Engineering, Jinan University, Guangzhou 510632, PR China

GRAPHICAL ABSTRACT

Schematic illustration for the synthesis of the POS@HNTs and the superhydrophobic POS@HNTs surfaces fabricated by spray-coating (the blue-colored globule represents water droplet on the surfaces).

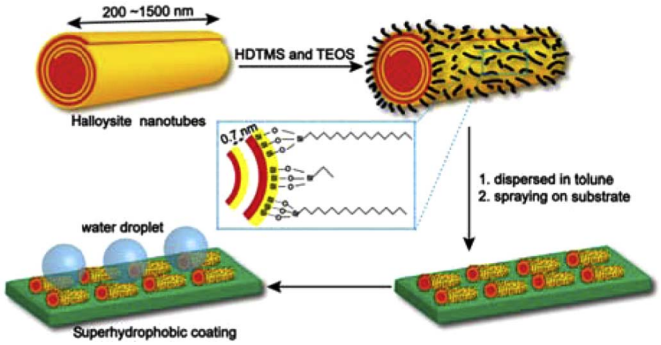

ARTICLE INFO

Keywords:
Halloysite
Hydrophobic
Silane
Separation
Surface modification

ABSTRACT

Superhydrophobic coatings with high water contact angles, ultralow sliding angles, excellent stability, oil/water separation, and self-cleaning functions were fabricated by spray-coating the suspensions of polysiloxane modified halloysite nanotubes (POS@HNTs) onto various substrates. The hydrophobic treatment of HNTs was performed by hydrolytic co-condensation of *n*-hexadecyltriethoxylsilane and tetraethoxysilane on the surfaces of the HNTs. A thick POS layer is located on the surfaces of the HNTs, which makes HNTs hydrophobic. The POS@HNTs were characterized using scanning electron microscopy, transmission electron microscope, Fourier transform infrared spectroscopy, X-ray diffraction analysis, X-ray photoelectron spectroscopy and thermogravimetric analysis. The effects of the ratio of silane and HNTs on the transparency, morphology, and wettability of the coatings were investigated. The transparency of the coating decreases with the increase in the silane loading. The water contact angles of the POS@HNTs coating increase with the increase in the silane loading, but the water sliding angles of the coatings are nearly independent on their ratio. The stability, oil/water separation, and self-healing capability of the coatings were also studied. The coatings on different substrates show high contact angle towards different liquid, e.g. 1 M HCl, 1 M NaOH, tea, and milk. Also, the POS@HNTs coated meshes can efficiently separate oils from water with high separation efficiency. In addition, the POS@HNTs coated gloves show a self-cleaning effect. All these results suggest that the POS@HNTs exhibit great potential for their application in waterproof materials, self-cleaning coating, and oil/water separation devices.

* Corresponding author.
E-mail address: liumx@jnu.edu.cn (M. Liu).
[1] These authors contributed equally to this work.

http://dx.doi.org/10.1016/j.cej.2017.09.023
Received 10 July 2017; Received in revised form 3 September 2017; Accepted 5 September 2017
Available online 07 September 2017
1385-8947/

1. Introduction

Superhydrophobic coating is a surface that is extremely difficult to wet. The contact angle of a water droplet on these surfaces exceeds 150° and the sliding angle of water is less than 10° [1]. The superhydrophobic effect is also referred to as the lotus effect, and a droplet impacting on these surfaces can fully rebound like an elastic ball. There are a lot of animals and plants in the nature that have the characteristics of superhydrophobicity, such as the surface of the lotus leaf, butterfly wings, and the leg of water strider [2]. The fabrication of the superhydrophobic surfaces has caused extensive attentions all over the world, which has become one of research hotspots in nanotechnology area [3]. The typical applications of the superhydrophobic surface include waterproof function, self-cleaning, anti-icing, corrosion resistance, and oil/water separation [1,4]. The superhydrophobic function is related to both chemical composition and structural characteristics of the surfaces which help trap a thin air layer that reduces attractive interactions between the solid surface and the liquid. For example, the lotus leaf surface possesses special micro/nanoscale binary structure and epicuticular wax crystalloids covered on its surface.

In order to prepare the superhydrophobic surfaces, many approaches have been employed to create appropriate roughness on a hydrophobic surface or modify a rough surface by low-surface-energy materials [5]. Phase separation, template printing method, electro/chemical deposition, electrospinning, laser and plasma etching, in situ growth, and so on can be classed into the first type. Xu et al. prepared a superhydrophobic surface with a CA of 163.0 ± 1.0° and SA of 7.0 ± 1.0° by casting the micellar solution of poly-(styrene)-*b*-poly (dimethylsiloxane) by vapor-induced phase separation [6]. An electrodeposition method for controllable fabrication of a superhydrophobic surface with a water CA of 162 ± 1° and a SA of 3 ± 0.5° was developed by deposition of nickel on copper substrate in the presence of (heptadecafluoro-1,1,2,2-tetradecyl)triethoxysilane [7]. On the other hand, superhydrophobic surfaces can be prepared by modifying a rough surface with low-surface-energy materials, i.e., solution immersion, thermal spraying, heat treatment, chemical vapor deposition, assembly and polymerization on the substrates. In order to introduction of low-surface-energy materials, a facile and rapid candle-soot deposition strategy to fabricate superhydrophobic coatings on porous materials of copper foam and various textile fabrics was recently studied [8]. Thermal spraying represents a simple, fast, and effective scale-up manufacturing methods for coating with large area. For example, spray-coating metal alkylcarboxylates of $Cu[CH_3(CH_2)_{10}COO]_2$ onto glass, aluminum, or other substrates can lead to a superhydrophobic surface with a static water CA of ~160° and a SA of 5° [9]. Superhydrophobic and transparent coatings onto paper can also be prepared by spraying alcohol suspensions of SiO_2 nanoparticles [10]. The development trend of the fabrication of superhydrophobic coating includes adopting facile method, improving mechanical durability, utilization of low cost raw materials, and realization of multifunction such as self-repairing [11].

Halloysite nanotubes (HNTs) are natural clay nanoparticles, with chemical formula of $Al_2Si_2O_5(OH)_4{\cdot}nH_2O$ [12,13]. HNTs exhibit a tube diameter of 15–50 nm and tube length of 300–1500 nm with aspect ratio of 6–100. HNTs have aluminum innermost and silicate outermost surfaces, which are positively and negatively charged respectively. The raw HNTs are hydrophilic and can be readily dispersed in water by mechanical stirring or ultrasonic treatment. The silanol and aluminols located in the inner side and edges of the HNTs are expected to react with silanes to change the surface into hydrophobicity [14,15]. For example, Yuan et al. modified and characterized the surfaces of HNTs with hydrophobic γ-aminopropyltriethoxysilane towards the application in polymer nanocomposites, enzyme immobilization and controlled release [16]. Lvov et al. modified HNTs inner and outer surfaces via sequential treatment using octadecylphosphonic acid and organosilane coupling agents. The octadecylphosphonic acid immobilized in HNTs lumen significantly increased the adsorption capacity of hydrophobic ferrocene molecules [17]. In 2013, Takahara et al. prepared low-energy HNTs surfaces by grafting with a long-chain alkylsilane, *n*-octadecyltrimethoxysilane (ODTMS). The surface-modified HNTs formed pincushion agglomerates on the surface of the liquid droplets, which create superhydrophobic surface similar to that of the plant gall surfaces [18]. Very recently, a durable underwater superoleophobic mesh was prepared by layer-by-layer (LBL) assembly of poly (diallyldimethylammonium chloride) (PDDA) and HNTs on a stainless steel mesh, which shows promising application in oil-water separation due to its stable oil-water performance, remarkable chemical and mechanical durability and the facile and eco-friendly preparation process [19]. However, there is no report on preparing HNTs superhydrophobic coating over large areas by a facile spraying method up to now.

In the present work, we first modified the HNTs surfaces by hydrolytic condensation of *n*-hexadecyltrimethoxysilane (HDTMS) and tetraethoxysilane (TEOS) to obtain polysiloxane modified HNTs (POS@HNTs). Then the superhydrophobic coatings were prepared by spray-coating the homogeneous POS@HNTs toluene suspension onto different substrates. The surface properties and morphology of HNTs before and after POS modification are characterized. The effects of the ratio of silane and HNTs on the transparency, morphology, and superhydrophobicity of the HNTs coatings were investigated. The stability, oil/water separation, and self-healing capability of the HNTs coatings were also studied. All the results suggest that the sprayed coated POS@HNTs exhibit superhydrophobic properties with oil/water separation and self-cleaning properties, which makes them good candidates in separation of oil from harsh water conditions and contamination prevention area.

2. Experimental

2.1. Raw materials

Halloysite nanotubes (HNTs) were purchased from Guangzhou Runwo Materials Technology Co., Ltd., China. Hexadecyltrimethoxysilane (HDTMS, ≥85%, Aladdin) and tetraethoxysilane (TEOS, Tianjin Damao Chemical Reagent Factory, China) were used and the chemical formulas of the silane and HNTs were shown in Fig. 1. Aqueous ammonia (25–28%, Tianjin Damao Chemical Reagent Factory, China), anhydrous ethanol (≥99.7%, Tianjian Fuyu Fine Chemical Co., Ltd., China) and toluene (≥99.5%, Tianjin HongDa Chemical Reagent Factory, China) were all of analytical grade. Glass slides (width × length × thickness: 25.4 × 76.2 × 1 mm, Sail Brand, China) were used as the main substrates for spray-coating. All of the other chemicals were used as received without further purification. Ultrapure water from Milli-Q water system was used to prepare the aqueous solutions.

2.2. Preparation of POS@HNTs

The POS@HNTs were prepared by triggering the hydrolytic condensation of silanes on the surface of HNTs [20]. Typically, 0.50 g of the HNTs, 0.25 g of the TEOS and 0.25 g of the HDTMS were dispersed in the mixture of 10 mL of anhydrous ethanol and 2 mL of aqueous ammonia. Then the solution was ultrasonicated for 30 min at room temperature. The hydrolytic condensation was first conducted at 60 °C for 30 min then at room temperature for 24 h under magnetic stirring. The resulting slurry is treated by centrifugation at 6000 rpm for 5 min and washing with ethanol for three times. After drying the products at 65 °C for 24 h, the POS@HNTs powder was finally obtained. The code of the POS@HNTs represents the percent of total weight of silanes to the weight of HNTs. For example, the 20% represented the weight of TEOS, HDTMS, and HNTs was 0.05, 0.05, and 0.5*g*. And the 60% represented the weight of TEOS, HDTMS, and HNTs was 0.15, 0.15, and 0.5*g*. The weight ratio of the TEOS:HDTMS was set as 1:1 (mole ratio of TEOS:HDTMS is 1.67:1) according to the reference [21]. TEOS acted as

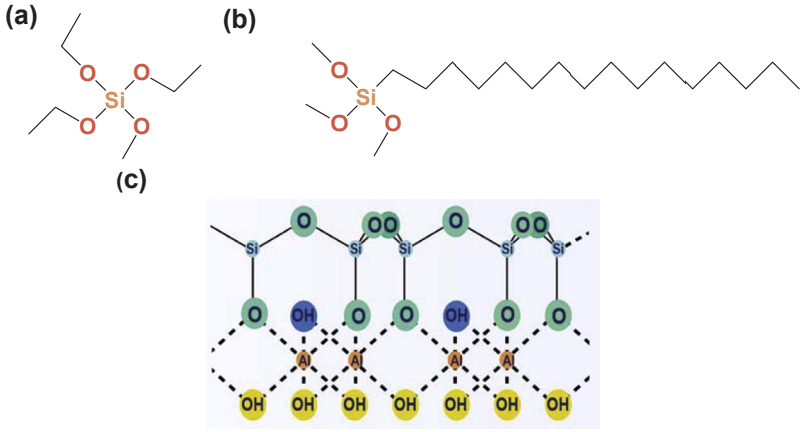

Fig. 1. Molecule structures of TEOS (a), HDTMS (b), and HNTs (c).

coupling agent which was beneficial to the hydrolytic condensation of HDTMS on the surface of HNTs.

2.3. Preparation of POS@HNTs coatings

The superhydrophobic coatings were fabricated by spray-coating the POS@HNTs toluene suspension onto the substrates. Glass slides were firstly washed with acetone and ethanol in turn, and then were soaked in deionized water twice, finally dried under a nitrogen gas flow. Typically, 0.05 g of POS@HNTs was dispersed in 7 mL toluene, following by ultrasonication for 30 min at room temperature. To avoid the sedimentation of POS@HNTs, the suspension was immediately spray-coated onto the glass slides. In order to achieve a uniform coating, the glass slides were fixed by tweezers, and the spray gun (iwata, WA-101) was placed perpendicularly to the glass slides from a 7–10 cm distance and moved from top to bottom with a constant speed. The nozzle diameter was 1.0 mm, and spraying air pressure was 0.29 MPa with flow rate of 100 mL/min. The thickness of the coatings can be controlled by spraying time. Other materials, including wood block, steel plate, cotton fabric, A4 paper, and nylon mesh (200-mesh) were also used as substrates for spraying according to the same procedure.

2.4. Characterization

2.4.1. Scanning electron microscope (SEM)

The surface microstructure of raw HNTs, POS@HNTs and the HNTs coating was observed using a field emission scanning electron microscope (FESEM) using a Zeiss Ultra 55 SEM machine at 5 kV. Before SEM observation, a layer of gold was sputtered.

2.4.2. Transmission electron microscope (TEM)

The morphology of raw HNTs and POS@HNTs was observed using a Philips Tecnai 10 TEM under an accelerating voltage of 100 kV. The dilute HNTs ethanol dispersions were dropped onto a carbon-film supported Cu grid and dried.

2.4.3. Fourier transform infrared spectroscopy (FTIR)

The FTIR spectra of the HNTs and POS@HNTs samples were measured using Nicolet iS50 FT-IR (Thermo Scientific, USA). Thirty-two consecutive scans were taken and their average was stored. Spectra were taken from 4000 to 400 cm^{-1}. The resolution of the wavenumber was 2 cm^{-1}.

2.4.4. X-ray diffraction analysis (XRD)

XRD of HNTs and POS@HNTs samples were obtained using X-ray diffractometer (D8, Bruker corporation) at room temperature. The CuKα radiation source was operated at 40 kV power and 40 mA current. The wavelength of the X-ray beam was 0.15418 nm, and the layer spacing of the sample was calculated according to the Bragg's equation. The scanning angle was from 5° to 70°.

2.4.5. X-ray photoelectron spectroscopy (XPS)

XPS of raw HNTs and 80% POS@HNTs was carried out by USA Thermo (ESCALAB250Xi). The atomic percent were given by the software.

2.4.6. Thermogravimetric analysis (TGA)

TGA was carried out with TA Q5000 from room temperature to 600 °C at a heating rate of 10 °C/min under N_2 atmosphere.

2.4.7. Transparency measurement

The transparency of the POS@HNTs coatings was shot by a camera and the quantitative analysis was determined on ultraviolet spectrophotometer (UV-2550, Shimadzu Instrument Ltd., Suzhou China) from 350 nm to 1000 nm wavelength.

2.4.8. Water contact angle measurement

WCAs of the samples were measured with a KRUSS drop shape analyzer DSA 100 instrument at 25.0 °C for the support and the injecting syringe as well. 10 μL water droplet vertically dropped from the syringe and then contacted the surface of the samples. The tilting angle of the tables was adjustable (0-360°) and allowed the subsequent measurement of SA at the same position on the sample. A minimum of three readings were recorded for each sample.

2.4.9. Separation of oil and water mixtures

The as-prepared 80% POS@HNTs coated nylon mesh (200-mesh) was fixed on the beaker. The diameter of the beaker was 47 mm. Water was dyed with methylene blue and oil (dichloromethane) was dyed with Oil Red O. The oil/water mixtures were poured onto the mesh. The separation was achieved by the weight of the liquids. The separation efficiency (η) was calculated according to $\eta = (V_1/V_0) \times 100\%$, where V_0 and V_1 are the volume of the oil before and after the separation process, respectively [22].

3. Results and discussion

3.1. Surface modification of HNTs by polysiloxane

The surface character of the POS@HNTs was firstly investigated. Fig. 2(A) shows the dispersion state of raw HNTs and POS@HNTs in water. It can be seen the raw HNTs are hydrophilic and can be readily dispersed in water via stirring. However, POS@HNTs are totally floating on the water, indicating their hydrophobic character after modification (Movie 1, Supporting information). Fig. 2(B) shows the

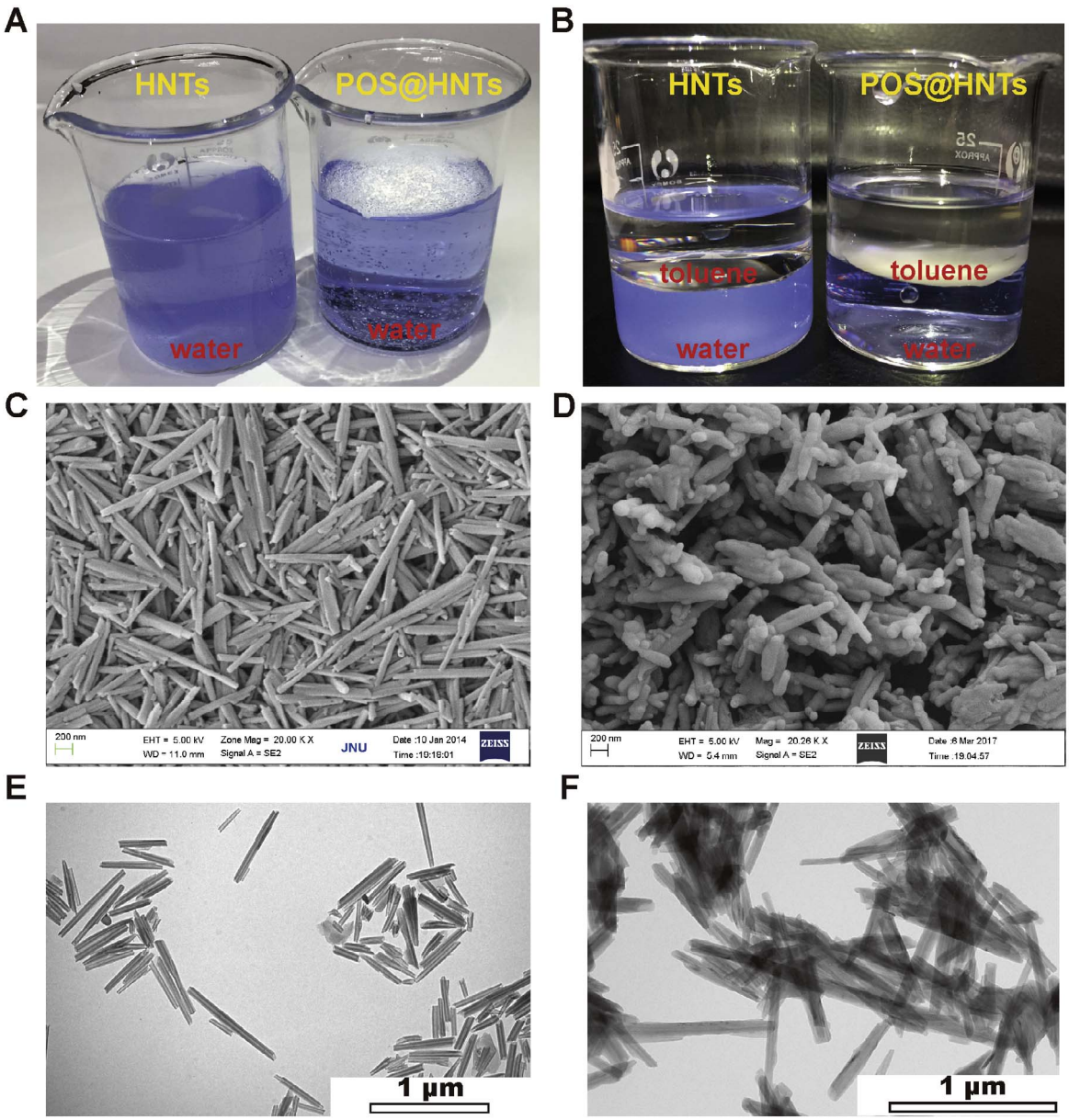

Fig. 2. The dispersion ability of HNTs and POS@HNTs in water (dyed by methyl blue) (A). The dispersion behavior of HNTs and POS@HNTs in a mixed oil/water liquid (B). SEM images of raw HNTs (C) and POS@HNTs (D). TEM images of raw HNTs (E) and POS@HNTs (F).

dispersion properties of the two HNTs in a toluene/water mixture. The top layer is toluene and the bottom layer is water. As expect, raw HNTs are hydrophilic and therefore located in the bottom layer of the toluene/water mixture. The POS@HNTs locate at the phase interface of toluene/water mixture due to the presence of hydrophobic alkyl groups on the surface of HNTs by silanes condensation and the incompatibility between silanes and water (Movie 2, Supporting information). This phenomenon is very consistent with previous reported silane modified HNTs [14,18,23]. The surfaces character of the POS@HNTs was further investigated by SEM and TEM observation. Fig. 2(C) and (D) compare the SEM morphology of the HNTs before and after modification. Raw HNTs show typical tubular morphology with smooth and sharp surfaces, while it is clear that the surfaces of POS@HNTs become rough. With aqueous ammonia as catalyst, hydrolytic co-condensation of HDTMS and TEOS occurred during silanization on the surfaces of HNTs. As a result, the surfaces of HNTs are coated with a dense layers of POS in thickness of ~44 nm rather than self-assembled monolayers [20,21]. A core-shell structure with HNTs as the core and polymer as the shell is formed. TEM results (Fig. 2(E) and (F)) also demonstrate that a layer of polymer located around the tubes. Also, the POS can warp the end of the tubes and can fill the lumen partly. This is attributed to that the silane polycondensation reaction can be performed both the aluminols and silanols groups. In contrast, the raw HNTs show very clean and smooth walls with empty lumen structure. Previous studies also showed that the warping of polymers always led to the changed HNTs morphology [24–26].

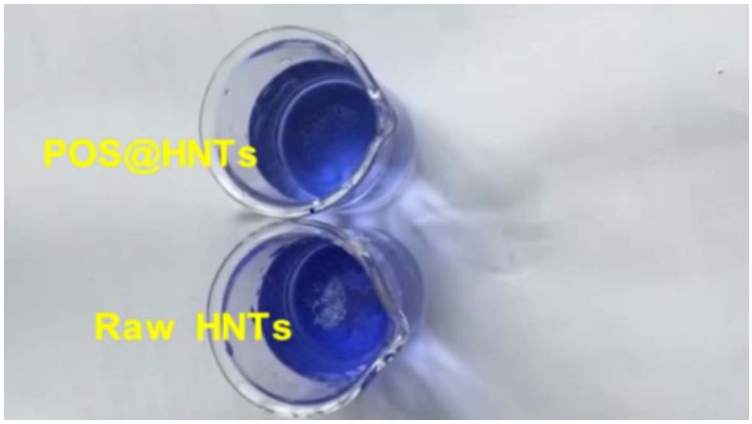

Movie 1.

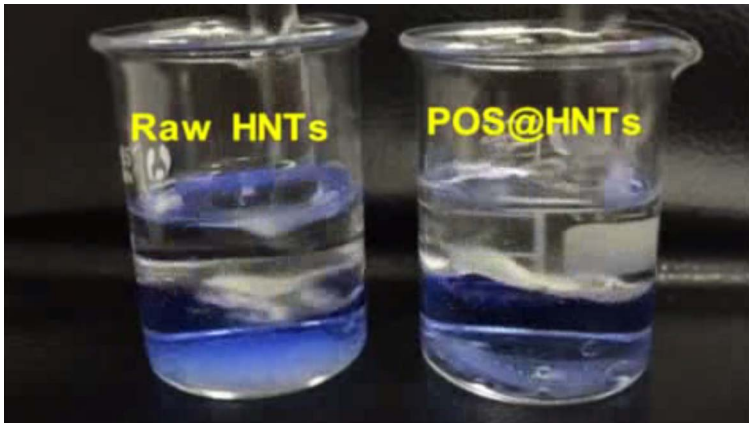

Movie 2.

Fig. 3A shows the FTIR spectra of raw HNTs and POS@HNTs. The spectrum of raw HNTs exhibits two characteristic peaks around 3695 cm^{-1} and 3620 cm^{-1} assigned to the Al_2OH stretching, a single Al_2OH bending band at 912 cm^{-1}, and bands at 1030 cm^{-1} and 790 cm^{-1} attributed to Si–O–Si stretching vibrations. Compared to the raw HNTs, POS@HNTs exhibit some new peaks, such as the aliphatic CH stretching at 2923 cm^{-1} and 2852 cm^{-1}, and the bending stretching of CH_2 vibration at 1467 cm^{-1}, CH_2 symmetrical scissoring in Si-CH_2 at 1408 cm^{-1} [27,28]. All of these new peaks suggest the presence of the POS moieties in the POS@HNTs. It also can be seen that the intensity of the peaks assigned to the organic moieties increases with the increase in TEOS and HDTMS loading. Similar FTIR result of POS modified nanoparticles was also found [21]. Fig. 3B shows the XRD patterns of raw HNTs and five different POS@HNTs. The raw HNTs show diffraction reflection at $2\theta = 11.7°$, 20.1°, 24.7°, and 35° assigned to (001), (020, 110), (002), (200, 130) plane, respectively. The peaks around 18° and 30° in the HNTs pattern are attributed to the impurity of alunite and quartz [29]. After POS modification, the diffraction peaks of HNTs have no obvious change. Therefore, it is suggested that the crystal structure of HNTs does not change and just a layer of hydrophobic groups is wrapped on the surface of HNTs. Fig. 3C compares the XPS spectra of raw HNTs and 80% POS@HNTs. The C 1s peak of carbon element of raw HNTs observed in the Fig. 3C was attributed to the impurities of the HNTs. It can be seen that the intensity of C 1s peak increases dramatically after POS modification. The percentage of C 1s increases from 17.95% (HNTs) to 60% (POS@HNTs), while the O 1s declines from 53.7% for HNTs to 25.5% for POS@HNTs. This strongly indicates the grafting of hexadecyl groups on the HNTs surfaces. The percentage of grafting of POS was further calculated by TGA. Fig. 3D shows the TGA curves of HNTs and POS@HNTs. The weight loss of raw HNTs before 100 °C is attributed to the evaporation of the adsorbed water in the sample. A sharp stage of weight loss of HNTs occurred in the temperature range of 400–500 °C, which is due to the dehydration of hydroxyl groups. The final weight loss of raw HNTs at 600 °C is 83.34%. In contrast, POS@HNTs start to decompose at ~300 °C with a salient point ~450 °C, which is attributed to the loss of the grafted POS. Afterwards, the POS@HNTs continue to lose weight to ~500 °C, which is also due to the dehydration of hydroxyl groups of HNTs. The percentage of grafting is about 14.81%. All these results demonstrated that the hydrophobic POS is successfully grafted onto the surfaces of HNTs [30,31].

3.2. Spray-coating of the POS-modified HNTs on glass substrate

The appearance of the POS@HNTs coating on glass slides is shown in Fig. 4A. Compared with the blank control glass slide, the glass slides coated with POS@HNTs with different mass ratio are semitransparent. The pattern under the glass can be seen in all samples. The transparency of the POS@HNTs coating is getting worse with the increasing concentration of grafting silanes from the images. The transparency is associated with the thickness and roughness of the coatings. The POS@HNTs coatings of each ratio were sprayed under the same condition and the thickness of the coatings of 5 POS-HNTs weight ratio showed almost no changes(~10 μm). However, the roughness has a great difference as shown in the Fig. 5. More aggregated HNTs are observed in the sample with higher silanes content, which indicates that the surfaces become rougher. The increased roughness results in increased light scattering and further leads to the decreased transparency of the POS@HNTs coatings. Also, the diameter of the POS@HNTs increases with increase in silane loading, which also leads to the increase in surface roughness. Fig. 4B compares the transparency of different coating by UV–vis spectroscopy. It also can be seen that as the concentration of the silanes increase, the transparency of the HNTs coating declines. However, all the coatings are semitransparent, which is convenient for observing the

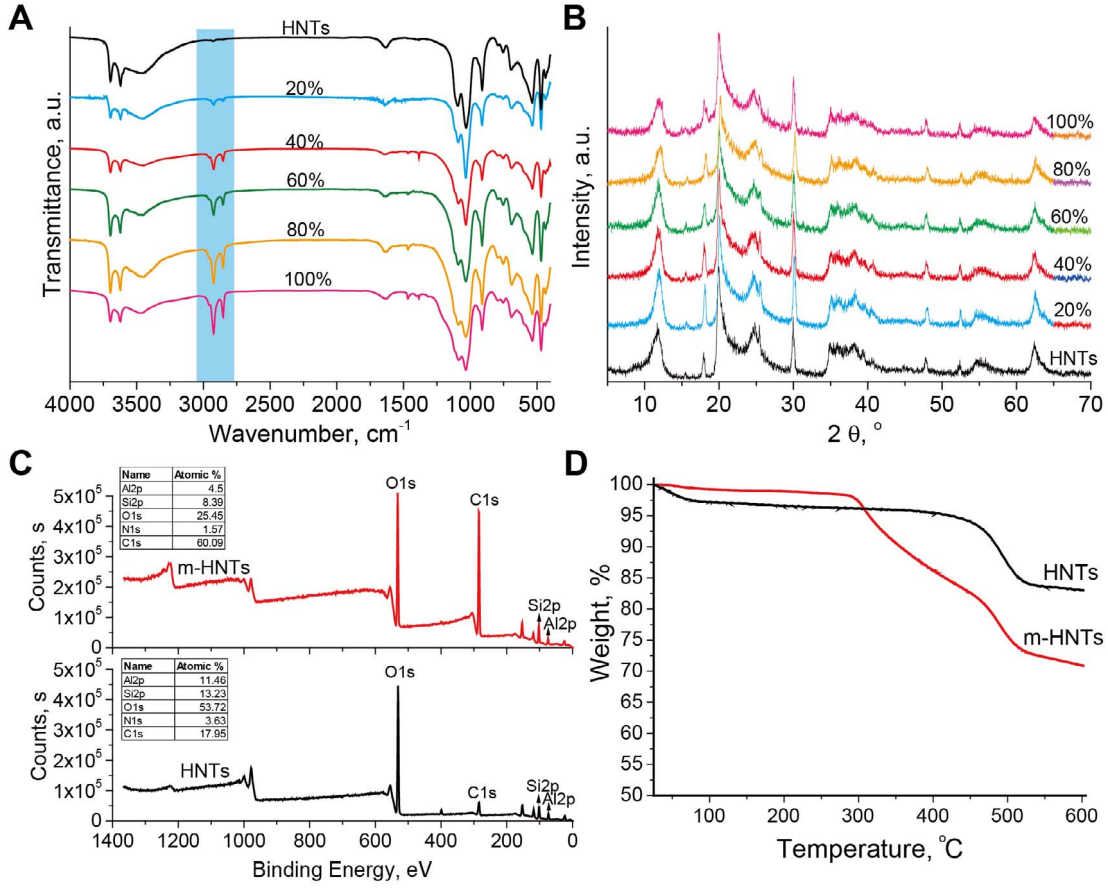

Fig. 3. IR spectra (A), XRD pattern (B), XPS survey (C), and TGA curves of the POS@HNTs.

objects behind the coating. In brief, all the HNTs coatings prepared by spraying are uniform without significant defects and large aggregates, which shows promising applications in many areas such as self-cleaning coating.

The surface morphology of the POS@HNTs coating is investigated by SEM. Fig. 5 shows the SEM images of different POS@HNTs coatings. Fig. 5A shows the images at magnification of 3k, and Fig. 5B shows the images at magnification of 10k. HNTs are randomly distributed on the surfaces of the glass slides. This unique structure is formed during the spraying process. A recent study described a spray-coating process that was utilized to create epoxy/HNTs nanocomposites with vertically aligned nanotubes. The alignment of HNTs changes from in-plane orientations toward the plane-normal direction with the increase of suspensions viscosity [32]. Since the viscosity of the HNTs suspensions in our work is low, which weakens the constraining of HNTs in as-sprayed films. So, the flow-induced orientation that developed at the nozzle exit is not maintained in the HNTs coatings. All POS@HNTs coatings show rough surfaces with dense and loose agglomerate composed with

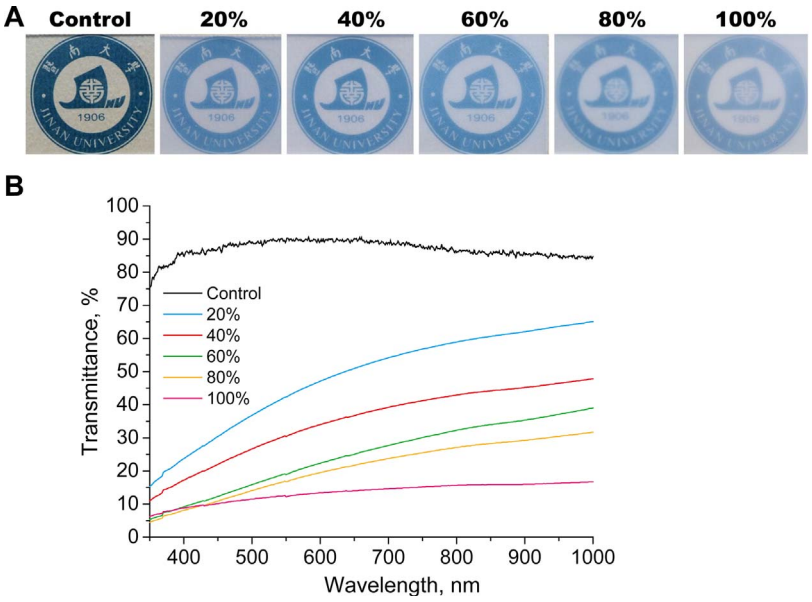

Fig. 4. Appearance (A) and transmittance (B) of the hydrophobic HNTs coatings on glass slides.

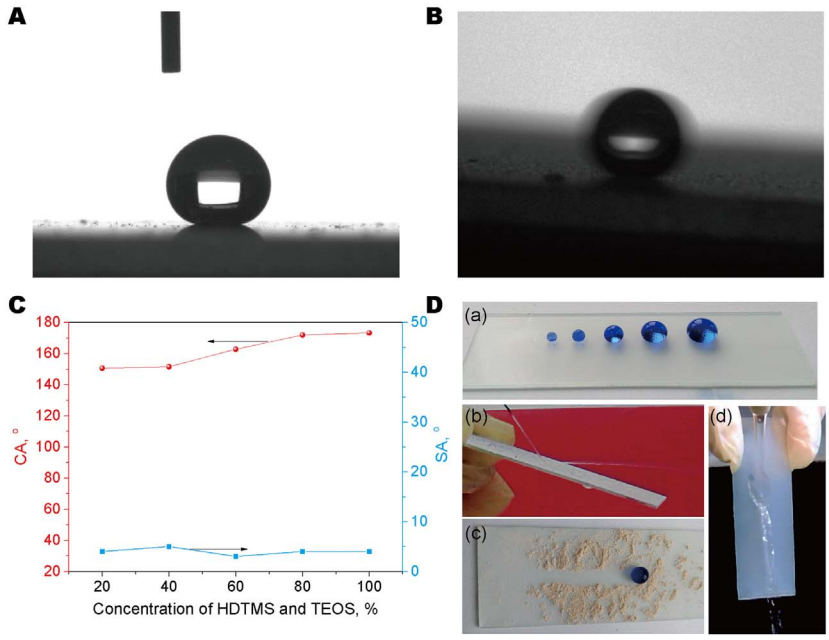

Fig. 5. SEM images of the hydrophobic HNTs coatings on glass slides with different POS loading.

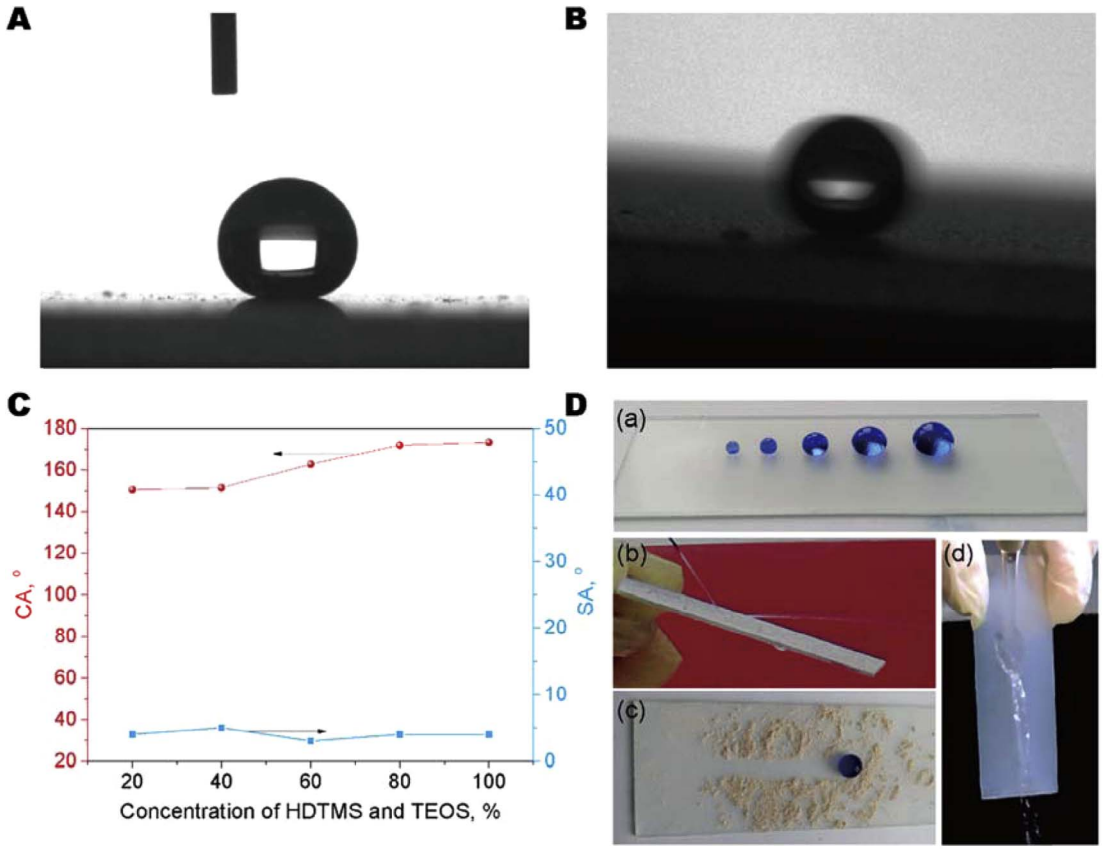

Fig. 6. Water contact angle (A) and slide angle (B) images of the hydrophobic POS@HNTs coatings. The CA and SA data of the hydrophobic POS@HNTs coatings (C) and the repellent water properties and self-cleaning properties of the hydrophobic 80% POS@HNTs coatings (D): (a) water droplets of different sizes on POS@HNTs coating; (b) a jet of water bounces off the POS@HNTs coating; (c) self-cleaning property of POS@HNTs coating; (d) a jet of faucet water applied on the POS@HNTs coating.

tubular-like nanoparticles. It is considered the rough surface can trap air which is beneficial to the improvement of the hydrophobicity. The surfaces roughness of the POS@HNTs coating increases with the increase of the silane loading, which consequently results in increase in the superhydrophobic properties. 80% POS@HNTs and 100% POS@HNTs coating surfaces are rougher, which is responsible for the decreased transparency and increased water repellent ability of these coatings illustrated below. The higher CA values of 80% and 100% POS@HNTs are due to the cooperation of the double structured higher surface roughness and the lower surface energy due to the grafted silanes [33]. Further experiment shows that repeating the spray-coating process at reduced silane loading could not lead to results that are similar to ones at higher silane loadings. Polysiloxanes layer around the HNTs at reduced silane loading is thin and cannot totally transfer HNTs

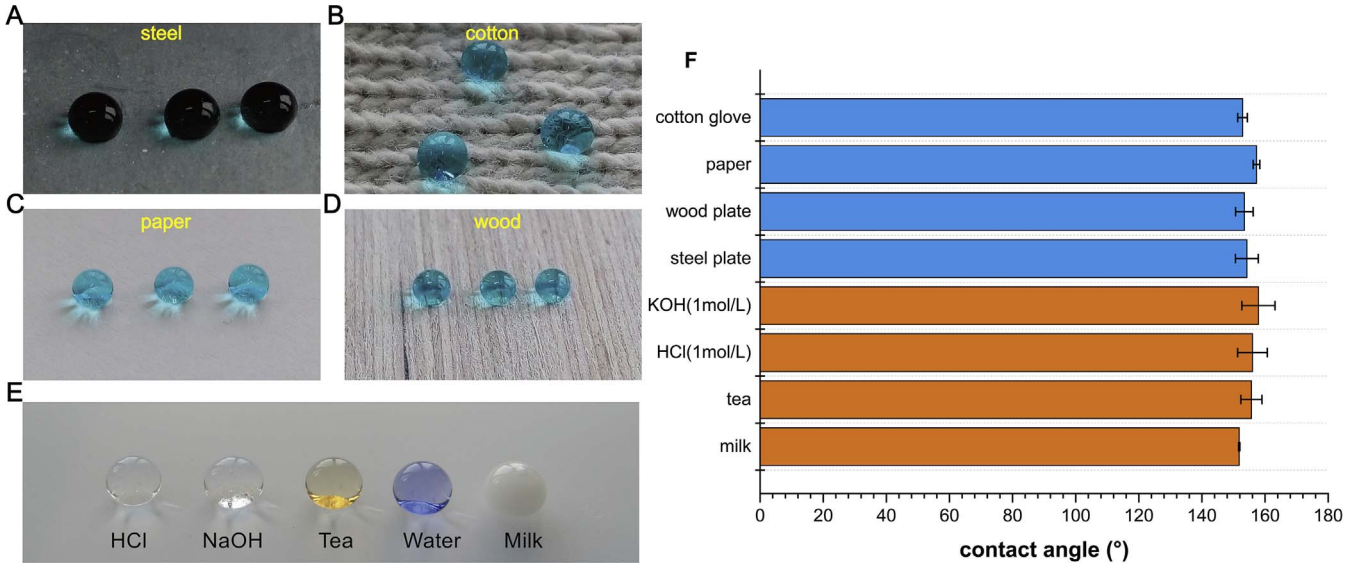

Fig. 7. Photographs of water (dyed with methylene blue) on the hydrophobic HNTs coating sprayed on different substrates: (A) steel; (B) cotton; (C) paper; (D) wood. The Photographs of 1 M HCl, 1 M NaOH, tea, water, and milk droplets on the hydrophobic HNTs coating (E). The water CAs on different substrates and different liquids on the hydrophobic POS@HNTs coating (F).

into superhydrophobic. Also, the aggregation brought by POS@HNTs with less silane loading on the coating is less and looser than that in the higher one.

The wetting properties of the prepared POS@HNTs coatings were then examined in detail. Fig. 6A shows the photo of the water droplets (10 μL) on the 100% POS@HNTs coatings. It can be seen that the water droplet is nearly spherical with a CA of 170°, suggesting the high water repellent ability of the coating. Fig. 6B shows the typical photo of a water droplet sliding on the POS@HNTs coating surface. The water droplets can easily roll off the POS@HNTs coatings even with slight vibration, indicating that the droplets on the coatings are in the Cassie-Baxter state. Fig. 6C shows the relationships of CAs and SAs of the HNTs coatings with the silane content. It is clear that all the surfaces exhibit superhydrophobicity with CA higher than 150°. The average water CAs of the 20%, 40%, 60%, 80%, 100% POS@HNTs coatings are 150.9°, 152.1°, 165.1°, 168.6°, 171.4°, respectively. Remarkably, the maximum water CA reaches to 174.4° corresponding to the 100% POS@HNTs coating. The growth of both the surface roughness and the grafting percentage are responsible for the rapid improvement of superhydrophobicity from 40% to 80% POS@HNTs coating. With further addition of silanes, the water CAs of 100% HNTs increase slightly, indicating that a uniform layer of silanes is formed at high silane content and the topography is rough enough. The water SAs of the coatings nearly are independent on silane loadings. The sliding angle measurements with 7 μL and 15 μL water droplet were also conducted and results showed that SA was almost no changed (5 ± 1°). This further suggests the excellent hydrophobic performance of the POS@HNTs coating. The repellent water properties and self-cleaning properties of the POS@HNTs coating are shown in Fig. 6D. The POS@HNTs coatings on glass are nonwettable by different size of water droplets (Fig. 6D-a). When the water column quickly hit the coatings, it bounces high to the air (Fig. 6D-b) (Movie 3, Supporting information). This is because the rough HNTs surface can trap air in pores and form air cushions which provide certain elasticity [34]. Moreover, powder dirt on the coatings can be efficiently washed off by water without any trace (Fig. 6D-c). It is considered that the air cushion in the rough surface leads to the decreased adhesion between the water droplet and surface, which make water freely move on the surfaces. The grafted silanes on the HNTs provide low surface energy of the coating. Fig. 6D-d shows a jet of faucet water applied on the POS@HNTs coating can also bounce off the surface without leaving a trace.

Movie 3.

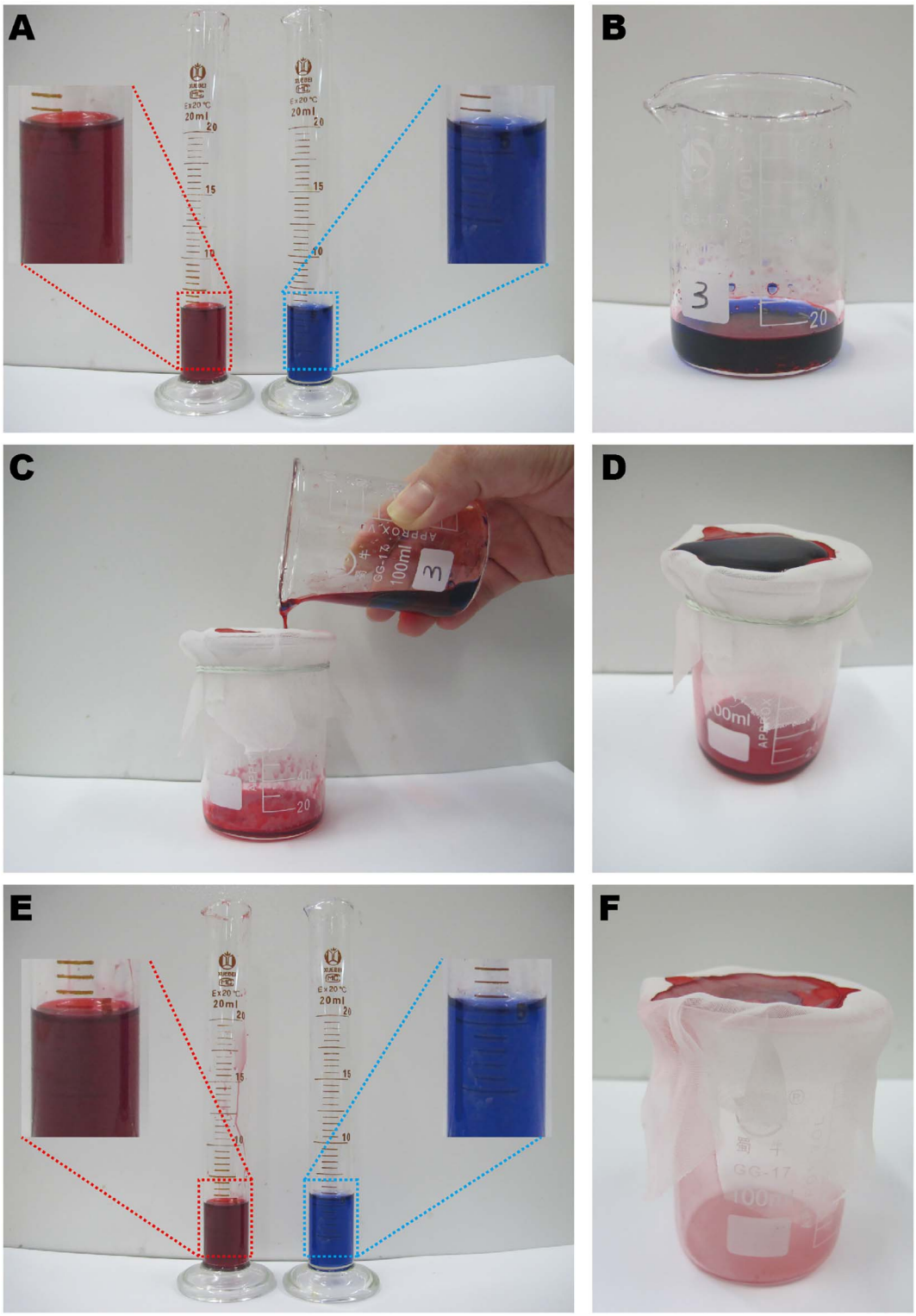

Fig. 8. The separation process of an oil (dichloromethane)/water mixture based on the hydrophobic HNTs coated mesh. Water is dyed with methylene blue and oil is dyed with Oil Red O (A) and then they are mixed before separation (B). The separation process of the oil/water mixture using the coated mesh (C-D). The water and oil volumes are nearly the same after separation (E). The appearance of the used mesh and beaker showing the residual oil and water on them after pouring into the cylinder in (F).

3.3. Anti-sticking, oil/water separation, and self-cleaning functions

Fig. 7A–D show the photos of the 80% POS@HNTs coating that sprayed on steel, cotton fabric, wood plate, and A4 paper. It can be seen the water droplet keeps high water CA nearly independent on the substrate type. The water CAs on the steel, cotton fabric, wood plate, and A4 paper is 154.2°, 152.9°, 153.4°, 157.3°, respectively (Fig. 7F). It should be mentioned that wood block, steel plate, cotton fabric, and A4 paper were used as received without further treatment. Therefore, the contact angles on above matte substrates are lower in comparison to ones on smooth glass substrates. These substrates with rough surfaces are hard to be coated with dense and thick POS@HNTs coatings, which

Fig. 9. Photos of uncoated (top) and hydrophobic HNTs coated (bottom) cotton gloves before and after being soaked in mud solution.

is responsible to the slight decrease in hydrophobic performance but they still maintain a water CA above 150°. The water droplet shows higher CAs on A4 paper than cotton and wood, because the latter two have higher surface roughness. The POS@HNTs coating is also non-wettable by various aqueous liquids such as 1 M HCl, 1 M NaOH, tea, milk, and the corresponding average water CAs is 156°, 157.9°, 155.7°, 151.8°. The CA of the milk is lower than other aqueous liquids, which is because fatty substance in milk has lower surface energy and stronger interaction with slianes.

The hydrophobic HNTs can be sprayed on a mesh to separate the mixture of oil and water. Fig. 8 show the procedure of oil/water separation process [35]. The coated mesh was firstly fixed at the top of the beaker. Then mixtures of 6 mL oil and 6 mL water were poured onto the mesh. Because of the high oleophilicity of the POS@HNTs, dichloromethane was absorbed on the mesh, gradually permeated through the mesh, and dropped into the beaker below. In contrast, water is retained over the mesh because of the superhydrophobicity of the POS@HNTs coating. The separation efficiency is high, nearly 6 mL water was recycled and no visible oil existed in the water, as shown in Fig. 8E. However, only ~83% oil is recycled because of the loss on the mesh and the beaker due to the adsorption (Fig. 8F). In addition, the recyclability of the modified mesh is good and the mesh can be used more than 5 times without decrease in the oil-water separation efficiency.

The POS@HNTs can also be coated on cotton gloves and cloth to keep their clean. Fig. 9 compares the whole process of untreated cotton gloves and POS@HNTs coated cotton gloves immersing into the mud water. It can be seen that the untreated cotton glove surface is covered with mud and become very dirty after taking out the mud water due to their hydrophilic character. In contrast, POS@HNTs coated glove are clean after taking out the mud water. This is attributed to the cotton gloves surface is sprayed with a layer of POS@HNTs, and a layer of hydrophobic protecting layer is formed on the cotton glove surface to achieve the hydrophobic effect. Also, it is expected that if the POS@HNTs are sprayed on clothes or shoes, they can also prevent dust and water effectively. Therefore, the typical applications of the prepared POS@HNTs coating include waterproof materials, self-cleaning coatings, and oil/water separation devices.

4. Conclusions

In summary, superhydrophobic coatings with high water contact angles, ultralow sliding angles, oil/water separation, and self-cleaning functions were fabricated by spray-coating the suspensions of POS modified HNTs onto various substrates. The hydrophobicity of HNTs was achieved by hydrolytic co-condensation of HDTMS and TEOS. A thick POS layer is located on the surfaces of HNTs, which leads to the transform from hydrophilic surfaces toward hydrophobic surfaces of HNTs. The transparency of the POS@HNTs coating decreases with the increase in the silane loading. The water CAs of the POS@HNTs coating increase with the increase in the silane loading, but the water SA of the coatings nearly is independent on their ratio. The POS@HNTs coatings on different substrates show high contact angle towards different liquid, e.g. 1 M HCl, 1 M NaOH, tea, and milk. The POS@HNTs coated meshes can efficiently separate oils from water with high separation efficiency. In addition, the POS@HNTs coated gloves show a self-cleaning effect. All these results suggest that the POS@HNTs exhibit great potential for their application in waterproof materials, self-cleaning coatings, and oil/water separation devices.

Acknowledgements

This work was supported by the National High Technology Research and Development Program of China (2015AA020915), the National Natural Science Foundation of China (51473069 and 51502113), and the Guangdong Natural Science Funds for Distinguished Young Scholar

(S2013050014606), Science and Technology Planning Project of Guangdong Province (2014A020217006), Guangdong Special Support Program (2014TQ01C127), the Pearl River S & T Nova Program of Guangzhou (201610010026), and Science and Technology Planning Project of Guangzhou (2017010160233).

References

[1] X.-M. Li, D. Reinhoudt, M. Crego-Calama, What do we need for a superhydrophobic surface? A review on the recent progress in the preparation of superhydrophobic surfaces, Chem. Soc. Rev. 36 (8) (2007) 1350–1368.
[2] L. Feng, et al., Super-hydrophobic surfaces: from natural to artificial, Adv. Mater. 14 (24) (2002) 1857–1860.
[3] Q. Wen, Z. Guo, Recent advances in the fabrication of superhydrophobic surfaces, Chem. Lett. 45 (10) (2016) 1134–1149.
[4] M. Nosonovsky, B. Bhushan, Superhydrophobic surfaces and emerging applications: non-adhesion, energy, green engineering, Curr. Opin. Colloid Interface Sci. 14 (4) (2009) 270–280.
[5] M. Ma, R.M. Hill, Superhydrophobic surfaces, Curr. Opin. Colloid Interface Sci. 11 (4) (2006) 193–202.
[6] N. Zhao, et al., Superhydrophobic surface from vapor-induced phase separation of copolymer micellar solution, Macromolecules 38 (22) (2005) 8996–8999.
[7] F. Su, K. Yao, Facile fabrication of superhydrophobic surface with excellent mechanical abrasion and corrosion resistance on copper substrate by a novel method, ACS Appl. Mater. Interfaces 6 (11) (2014) 8762–8770.
[8] G. Ju, et al., Chemical and equipment-free strategy to fabricate water/oil separating materials for emergent oil spill accidents, Langmuir 33 (10) (2017) 2664–2670.
[9] W. Wu, et al., Spray-coated fluorine-free superhydrophobic coatings with easy repairability and applicability, ACS Appl. Mater. Interfaces 1 (8) (2009) 1656–1661.
[10] H. Ogihara, et al., Simple method for preparing superhydrophobic paper: spray-deposited hydrophobic silica nanoparticle coatings exhibit high water-repellency and transparency, Langmuir 28 (10) (2012) 4605–4608.
[11] X. Tian, T. Verho, R.H.A. Ras, Moving superhydrophobic surfaces toward real-world applications, Science 352 (6282) (2016) 142–143.
[12] Y. Lvov, et al., Halloysite clay nanotubes for loading and sustained release of functional compounds, Adv. Mater. 28 (6) (2016) 1227–1250.
[13] M. Liu, et al., Recent advance in research on halloysite nanotubes-polymer nanocomposite, Prog Polym. Sci. 39 (8) (2014) 1498–1525.
[14] M. Liu, et al., Functionalized halloysite nanotube by chitosan grafting for drug delivery of curcumin to achieve enhanced anticancer efficacy, J. Mater. Chem. B 4 (13) (2016) 2253–2263.
[15] J. Yang, et al., Enhanced therapeutic efficacy of doxorubicin for breast cancer using chitosan oligosaccharide-modified halloysite nanotubes, ACS Appl. Mater. Interfaces 8 (40) (2016) 26578–26590.
[16] P. Yuan, et al., Functionalization of halloysite clay nanotubes by grafting with γ-aminopropyltriethoxysilane, J. Phys. Chem. C 112 (40) (2008) 15742–15751.
[17] W.O. Yah, A. Takahara, Y.M. Lvov, Selective modification of halloysite lumen with octadecylphosphonic acid: new inorganic tubular micelle, J. Am. Chem. Soc. 134 (3) (2012) 1853–1859.
[18] H. Wu, et al., Robust liquid marbles stabilized with surface-modified halloysite nanotubes, Langmuir 29 (48) (2013) 14971–14975.
[19] K. Hou, et al., Durable underwater superoleophobic PDDA/halloysite nanotubes decorated stainless steel mesh for efficient oil–water separation, Appl. Surf. Sci. 416 (2017) 344–352.
[20] L. Li, et al., Roles of silanes and silicones in forming superhydrophobic and superoleophobic materials, J. Mater. Chem. A 4 (36) (2016) 13677–13725.
[21] Y. Zhang, J. Zhang, A. Wang, From Maya blue to biomimetic pigments: durable biomimetic pigments with self-cleaning property, J. Mater. Chem. A 4 (3) (2016) 901–907.
[22] J. Li, et al., Superhydrophobic meshes that can repel hot water and strong corrosive liquids used for efficient gravity-driven oil/water separation, Nanoscale 8 (14) (2016) 7638.
[23] B. Guo, et al., Structure and performance of polyamide 6/halloysite nanotubes nanocomposites, Polym. J. 41 (10) (2009) 835.
[24] C. Chao, et al., Surface modification of halloysite nanotubes with dopamine for enzyme immobilization, ACS Appl. Mater. Interfaces 5 (21) (2013) 10559–10564.
[25] M. Liu, et al., Chitosan–halloysite nanotubes nanocomposite scaffolds for tissue engineering, J. Mater. Chem. B 1 (15) (2013) 2078–2089.
[26] J. Zhang, et al., Poly (methyl methacrylate) grafted halloysite nanotubes and its epoxy acrylate composites by ultraviolet curing method, J. Reinforced Plastics Composites 32 (10) (2013) 713–725.
[27] Schué, F., First International Congress on Adhesion Science and Technology: Festschrift in Honor of Dr KL Mittal Edited by WJ Van Ooij and HR Anderson, Jr, Zeist, The Netherlands VSP BV, 1998 pp 898, price ISBN 90-6764-291-6. Polymer International, 2000. 49(8): p. 903-904.
[28] Laboratories, S.R., Sadtler Handbook of Reference Spectra - IR. 1978: Sadtler Research Laboratories; HiNGE CRACKED edition (August 1978).
[29] P. Pasbakhsh, G.J. Churchman, J.L. Keeling, Characterisation of properties of various halloysites relevant to their use as nanotubes and microfibre fillers, Appl. Clay Sci. 74 (2013) 47–57.
[30] B. Mu, M. Zhao, P. Liu, Halloysite nanotubes grafted hyperbranched (co)polymers via surface-initiated self-condensing vinyl (co)polymerization, J. Nanoparticle Res. 10 (5) (2008) 831–838.
[31] H. Zhang, et al., High-efficiency grafting of halloysite nanotubes by using π -conjugated polyfluorenes via “click” chemistry, J. Mater. Sci. 50 (12) (2015) 4387–4395.
[32] K. Song, et al., Spray-coated halloysite-epoxy composites: a means to create mechanically robust, vertically aligned nanotube composites, ACS Appl. Mater. Interfaces 8 (31) (2016) 20396.
[33] D. Xu, et al., Fabrication of superhydrophobic surfaces with non-aligned alkyl-modified multi-wall carbon nanotubes, Carbon 44 (15) (2006) 3226–3231.
[34] S.A. Mahadik, et al., Durability and restoring of superhydrophobic properties in silica-based coatings, J. Colloid Interface Sci. 405 (2013) 262–268.
[35] Z. Xue, et al., A novel superhydrophilic and underwater superoleophobic hydrogel-coated mesh for oil/water separation, Adv. Mater. 23 (37) (2011) 4270–4273.